Henrik O. Saldner
Division of Experimental Mechanics
Luleå University of Technology
S-97187 Luleå, Sweden
e-mail: henrik@mt.luth.se

Calibrated Noncontact Exciters for Optical Modal Analysis

Two types of exciters were investigated experimentally. One of the exciters uses a small permanent magnet fastened on the object. The force is introduced by the change in the electromagnetic field from a coil via an air gap. The second exciter is an eddy-current electromagnet one. The amplitude of the forces from these exciters are calibrated by using dynamic reciprocity in conjunction with electronic holography. These forces strongly depend upon the distance between the exciter and the object.

INTRODUCTION

Experimental modal analysis has become more important as structures and materials become more sophisticated. Modal analysis refers to the process of determining modal parameters like frequencies, damping factors, and modal vectors (mode shapes) Ewins, (1984). Modal parameters may be determined analytically or by experiments. The experiments are often used to verify an analytical model. If such a model does not exist, the experimentally determined modal parameters can serve as a model of the object. The modal parameters may be used for structural modifications or to explain the dynamics of the structure.

If the object is stiff and heavy, accelerometers or other contacting experimental techniques can often be used. For thin and weak structures the object behavior is, however, changed by the mass loading from accelerometers. A noncontact technique is then preferred. Today, there are effective noncontacting techniques available such as laser Doppler vibrometers and electronic holography techniques. A review of recent developments in electronic holography techniques is described in Løkberg (1993).

In most experiments with stiff and heavy objects, the object is forced to vibrate, either from an impact of the hammer or from a frequency controlled exciter. If the object is thin and weak, the exciter should be of the noncontacting type. Different types of such exciters are loudspeakers, eddy-current exciters, and coils with a permanent magnet fastened to the object. In this study eddy-current and permanent magnet exciters were calibrated using dynamic mechanical reciprocity and electronic holography (EH). The force from the exciters were calibrated using reference objects and a quartz force transducer.

Two examples of optical modal analysis are also presented. Body modes of vibration of a violin were analyzed using EH. Modes of vibration of a plate were analyzed using electronic shearog-

Received November 24, 1994; Accepted September 18, 1995.
Shock and Vibration, Vol. 3, No. 2, pp. 107–115 (1996)

CCC 1070-9622/96/020107-09

raphy (ES) in the second example. ES is a special version of EH and measures the spatial derivative of the out-of-plane deformation field. Shearography is often used for nondestructive testing (Hung, 1974). This technique has recently been extended by Mohan et al. (1994) to include vibration studies.

NONCONTACT EXCITERS

Two types of exciters were studied experimentally. Both use forces introduced by changes in an electromagnetic field of a coil and a permanent magnet. The first type, called type I, has the magnet fastened onto the object. For the eddy-current type, type II, the magnet and the coil are mounted as one unit separated from the object [compare Fig. 1(a) and (b)].

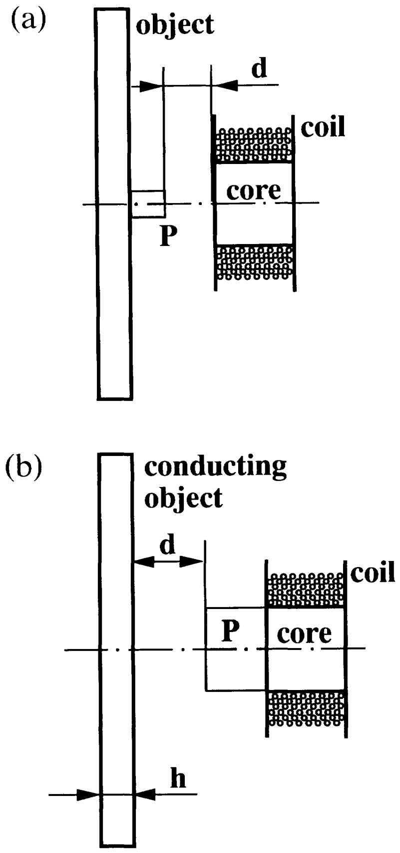

FIGURE 1 Two noncontact exciters. (a) Type I has a small permanent magnet, P, fastened onto the object. (b) Types II is an eddy-current electromagnet exciter with the coil and the magnet as one unit.

Permanent Magnet and Coil (Type I)

Figure 1(a) shows the design of the exciter. A small permanent magnet is waxed onto the surface of the structure. A coil is placed close to the permanent magnet with an air gap *d*. The stationary magnetic field from the permanent magnet interacts with the varying electromagnetic field from the coil that causes the desired out-of-plane force.

This force depends upon the strength of the permanent magnet and the strength of the electromagnetic field from the coil. Because the magnetic field from the coil is proportional to the current in the coil, the force is proportional to the voltage of the driving signal generator at a constant frequency. The relation between voltage E and current I is in the $j\omega$ method related as $(j\omega L + R) I = E$, where ω is the angular frequency and j is the square root of -1. L and R are the inductance and the resistance of the coil, respectively. Thus, the force will decrease with increasing frequency. If $R \gg \omega L$, the force will be approximately independent of the frequency. The frequency of the force is the same as that of the current through the coil.

The permanent magnet fastened onto the surface of the object gives a mass loading and should be as small as possible. A cylindrical 0.35-g permanent magnet, which sticks to an iron plate with a force of about 1 N, was used in the experiments (length 3.5 mm, diameter 3.5 mm). Two different coils were used in the present experiments: one without core and dimensions (length 16 mm and diameter 12 mm), and one with an iron core with about 40 windings and dimensions (length 3.0 mm and diameter 12 mm).

Eddy-Current Electromagnet Exciters (Type II)

The eddy-current electromagnet exciter is shown in Fig. 1(b). A sinusoidal current in the coil will introduce harmonically varying eddy currents in the conducting object. The electromagnetic field generated by the eddy currents will interact with the stationary field from the permanent magnet and give rise to a force. The principle of this exciter can easily be verified in the following way: place a coil on one side of an object, a thin conducting plate. A force will be introduced in the object if a permanent magnet is placed on the other side of the plate.

The eddy current in the object decreases exponentially with depth from the surface. The skin depth δ is defined as the depth in the material where the electromagnetic wave is reduced to 1/e ($\approx$0.37) of its initial amplitude. For good conductors the skin depth is formulated in Jackson (1975) as

$$\delta = \sqrt{\frac{2}{\mu\omega\sigma'}} \tag{1}$$

where ω is the angular frequency and μ and σ are the permeability and the conductivity of the object material, respectively. If δ is much less than the thickness h of the object, the force will be independent of h. For aluminum, δ is about 8 mm for frequencies in the range of 100 Hz. In most experiments, the forces will depend upon the thickness of the object and a calibration of the force is needed for different object thicknesses. The present exciter has a permanent magnet that sticks to an iron plate with a force of about 40 N and with about 600 windings. The dimensions are length 12.5 mm and diameter 13.2 mm. The magnet is glued to the iron core of the coil in a single unit.

EH

The EH system uses a four frame, phase stepped speckle interferometric technique. It offers efficient ways to measure fields of deformation and allows the deformation to be visualized in real time. Names such as electronic speckle pattern interferometry (ESPI), electrooptic holography, and TV holography are commonly found in the literature for similar techniques. The system used was developed at United Technologies Research Center (UTRC) in the U.S. by Stetson (1990) and Stetson et al. (1989) (see Fig. 2). The object is illuminated by a 500-mW frequency doubled Nd: YAG laser (wavelength 532 nm). The image of the object interferes with a smooth reference beam from an optical fiber onto a CCD camera.

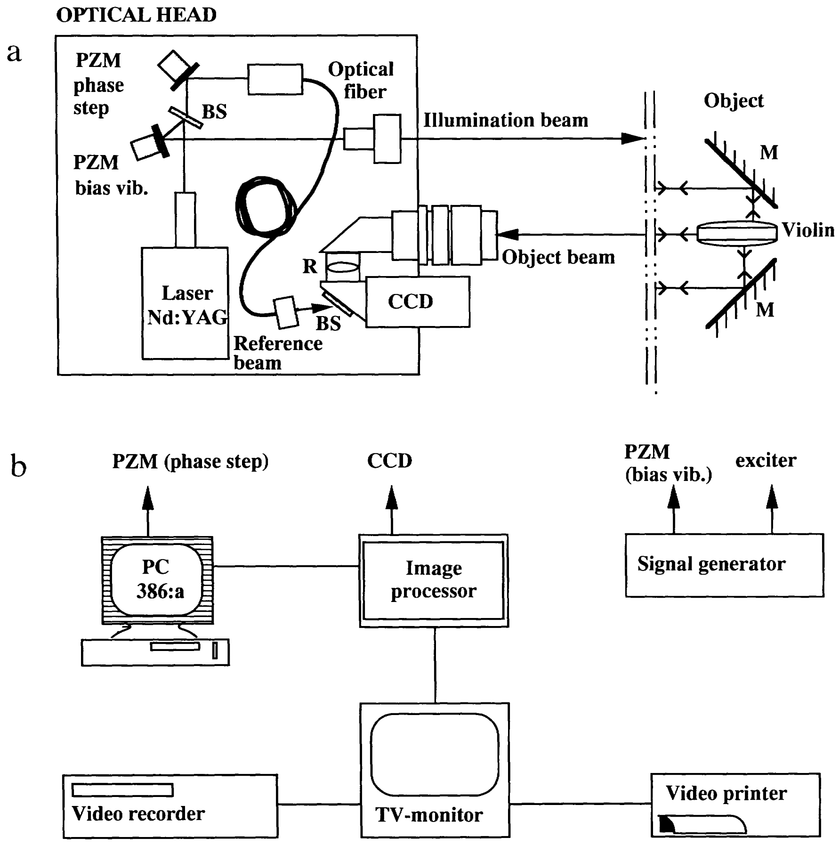

FIGURE 2 (a) The optical head of the electronic holography system and the object arrangement used for the violin experiment. Three sides of the violin are studied simultaneously via mirrors. (b) Electronic components of the system.

A piezo mounted mirror (PZM) introduces optical phase steps of 90° between subsequent images. Four consecutive images are treated by an image processor and presented as high quality interferograms on a monitor in real time (30 frames/s). A host computer controls the image processor and the phase stepping PZM. To grasp the interferograms, the object has to be excited at single frequencies or by frequency sweeps.

From an interferogram it is not possible to say if the antinode is a "hill" or a "valley," that is, in-phase or out-of-phase compared to other antinodes. A second PZM is therefore used to find this important phase relation. The mirror is set to vibrate at the same frequency, amplitude, and phase as some part of the object. This is often called a bias vibration. This part of the object will then act as a new nodal line.The real nodal lines will be given the number of fringes that corresponds to the amplitude of the bias vibration of the PZM. By switching the bias vibration on and off, the phase of the antinodes can be determined from the increase or decrease of the number of fringes in each antinode. This facility is needed for the study of complicated modes or when the object is imaged via mirrors. Numerical evaluation of the vibration amplitude distribution can also be performed by recording three interferograms, without bias, with positive bias and with negative bias, together with a postprocessing routine. The details are described in Stetson and Brohinsky (1988).

To reduce the speckle noise and thus improve the quality of the interferograms, speckle averaging is possible. A number of interferograms are averaged to produce the final interferogram. Each interferogram is given a slightly different illumination direction to get a different speckle pattern.

RECIPROCITY AND CALIBRATION OF EXCITERS

In static loading of a linear elastic body with a single force, the relation between load and deformation is given by Maxwell's reciprocal relation. Maxwell's reciprocal relation is described in Fung (1965). The equation is usually written as

$$\frac{\mathbf{P}_1'}{\mathbf{u}_2'} = \frac{\mathbf{P}_2''}{\mathbf{u}_1''}, \tag{2}$$

where the loads $\mathbf{P}_i$ can be either a force or a couple and the corresponding deformations $\mathbf{u}_i$ are a displacement or a change in slope, respectively ($'$ indicates first and $''$ the second loading and the index numbers refers to position). With a known reference and $\mathbf{P}_1'$ and measured deformations $\mathbf{u}_2'$ and $\mathbf{u}_1''$, the unknown load $\mathbf{P}_2''$ can be determined. Reciprocity for a dynamically loaded system is usually formulated in a similar way as Maxwell's reciprocal relation for static loading (Wolde, 1973). Here, however, other corresponding pairs of variables are used. For mechanical reciprocity we may have force F (N) and translation velocity v (m/s). The experiments with EH are performed at a single frequency where the velocity amplitude is proportional to the measured amplitude of the vibration.

This reciprocity relation has been used to calibrate the amplitude of the force for both types of exciters. A type I exciter was first calibrated with a quartz force transducer on a stiff and heavy object. This calibrated exciter was then used as the reference in the reciprocal experiment. A Brüel & Kjær force transducer (type 8200) was used in the experiments.

The reciprocal calibration is performed in the following way: a reference force amplitude is applied to a plate as the known load $\mathbf{P}_1'$ at position 1. The amplitude of the vibration field $\mathbf{u}(x, y)'$ of the whole plate is measured using EH. A second force $\mathbf{P}_2'$, the one we want to calibrate, is applied to the plate at position 2 and the second deformation field $\mathbf{u}(x, y)''$ is measured. The two measured deformation fields include the deformations at position 1 and 2, that is, $\mathbf{u}_2'$ and $\mathbf{u}_1''$, respectively. If the vibration and the force are in phase (or out of phase) the numerical amplitude values from the experiments can be used directly in Eq. (2) to give the unknown quantity $\mathbf{P}_2''$. If the object has a low mechanical damping and if the frequencies are separated from an eigenfrequency, this phase condition will be fulfilled. Two similar aluminum plates of different thicknesses were used as objects with dimensions 120×90 mm^2 and thicknesses 0.7 and 2.0 mm. The damping factor ζ of the plates as experimentally determined to be $\zeta < 0.006$ from the sharpness of the lower resonances as in Thomson (1988).

The type I exciter can be used on different object materials according to this calibration. But the type II eddy-current exciters have to be calibrated for each material and thickness.

RESULTS

An exciter of type I was first calibrated with a force transducer for frequencies between 200 and

2000 Hz. The result is shown in Fig. 3(a). For increasing frequency the force gets smaller for constant driving voltage and distance d. The dependencies of the distance d (see Fig. 1) was measured using the aluminum plate. Figure 3(b) and (c) show this dependence for a type I exciter; the coil in (b) has no iron core. The distance d can become negative [see Fig. 1(a)]. In Fig. 3(c), a coil with an iron core is used. Due to the number of windings of the second coil and the iron core, the force gets larger for this exciter. A 0.35-g permanent magnet is used in graph (b) and (c). Both the coils were also tested below and above the resonance of the object. An unwanted behavior is found for short distances d, most clearly seen for the coil with iron core [Fig. 3(c)]. The reason for this peculiar behavior above and below object resonance is the effect of motion of the permanent magnet. Below resonance the object deformation and the force will be in phase and above they will be out of phase for low damped objects. The moving permanent magnet influences the force differently in and out of phase. For a larger distance d, this effect can be neglected and both coils work better, say for distances d > 1.5 mm. Each new coil has to be analyzed to get the smallest working distance. From Fig. 3(b) and (c) it is tempting to use coils only without iron cores, but they need higher electrical power to get the same amplitude of the force. (Even if the voltage is less in graph (b), in (c) the power is much higher.)

Results for the eddy-current exciter are shown in Fig. 3(d) for a 0.7-mm aluminum plate. The $(d + \text{constant})^{-3}$ form of the graph is as expected due to the cubic decrease with distance of the electromagnetic field for a dipole. The unwanted behavior described above does not exist for the type II exciters. If a 2.0-mm aluminum plate is used instead, the force will increase 2.2 times.

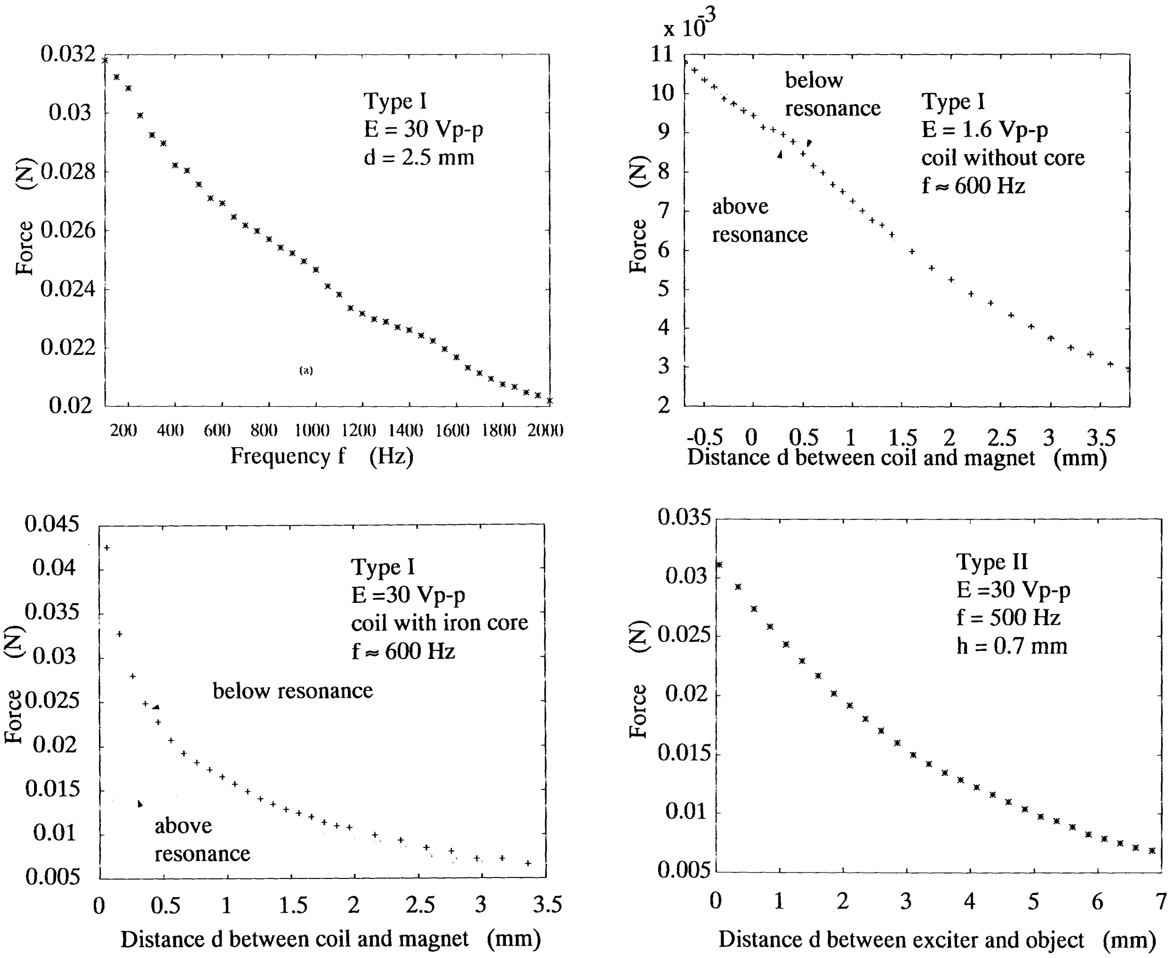

FIGURE 3 (a) Force vs. frequency for the reference exciter, type I. (b) and (c) Force vs. distance d [see Fig. 1(a)], for two different coils with and without iron core, type I. (d) Force vs. distance d [see Fig. 1(b)], for the eddy-current electromagnet exciter type II for a 0.7-mm aluminum plate.

OPTICAL MODAL ANALYSIS

Short comments from two optical modal analysis experiments, where these exciters were used, are presented below.

Body Modes of a Violin

The first experiment concerns whole body vibrations of a violin. Because the material is wood, a type I exciter was used. The magnet is waxed to the treble side of the bridge. Three sides of the instrument are observed simultaneously via mirrors (compare Fig. 2 and the interferograms in Fig. 4). An interferogram presented live on the monitor looks as shown in Fig. 4. Each fringe seen on the surface of the violin model connects points that are vibrating with equal amplitude. Going from one such fringe to the next gives a change of about 0.13 μm in amplitude. The brightest part in the interferogram are nodal lines that have zero vibration amplitude.

The optical modal analysis was conducted to seek answers to some questions formulated by Jansson et al. (1994). One of the questions was: Are basic low-frequency vibration modes of a musically superior instrument different from those of an inferior violin? The details of the experiments are given by Jansson et al. (1994). The lower modes are found to be quite equal even if differences in shape were observed. A noticed difference was how easy the violin was excited. It was easier to get large vibrations in a musically superior instrument. Figure 4(a) shows a torsion mode at 430 Hz. The 465-Hz mode in Fig. 4(b) is quite complicated. By the use of the bias vibration mirror it was found that the largest antinodes in the top (the right part of the image) and the antinode in the back are moving out of phase. Notice that the ribs vibrate considerably.

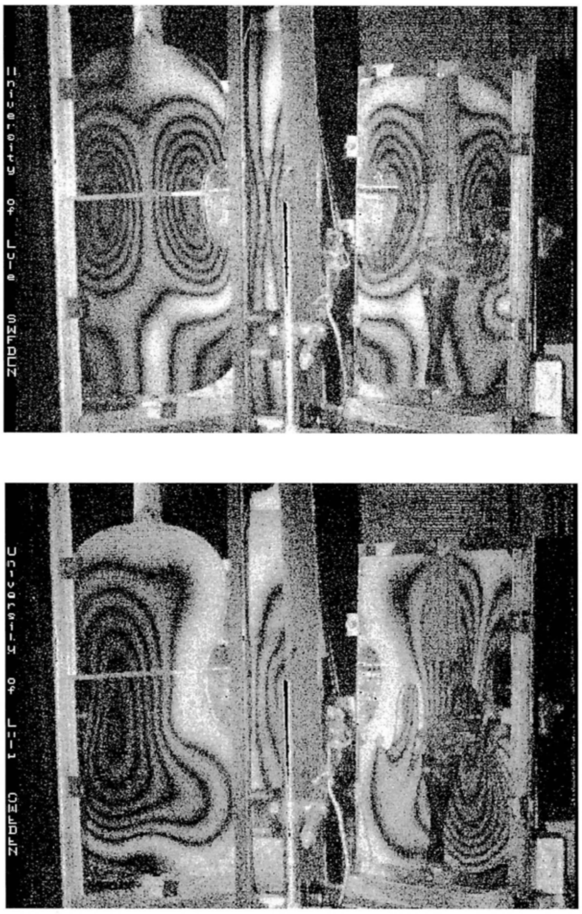

FIGURE 4 Modal analysis of a violin using electronic holography (EH). Three sides of the violin are studied simultaneously: the back plate to the left, the top plate to the right, and one side of the ribs in the middle of the image. Interferograms of two vibration modes: (a) at 430 Hz and (b) at 465 Hz.

Modal Analysis using ES

ES is a version of EH where the spatial derivative of the out-of-plane deformation field, the slope change, is measured (Mohan et al., 1994). The experimental arrangement is shown in Fig. 5. A type II exciter is used at the center of the plate on the back side. The object is illuminated by a laser light at near normal incidence. It is imaged onto the photo sensitive surface plate of a CCD camera via a piezo electrically driven mirror,

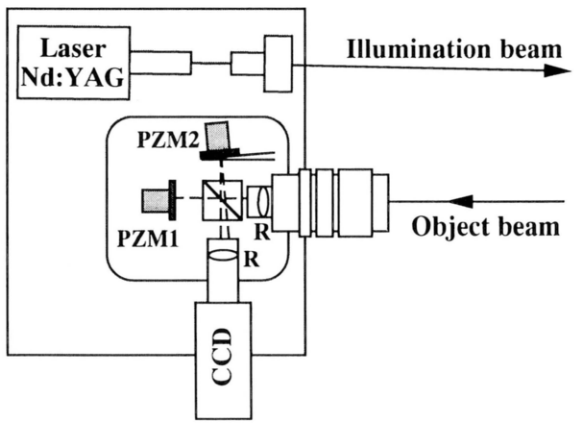

FIGURE 5 The optical head of the electronic shearography setup for measurements of a spatial derivative of the amplitude of vibration.

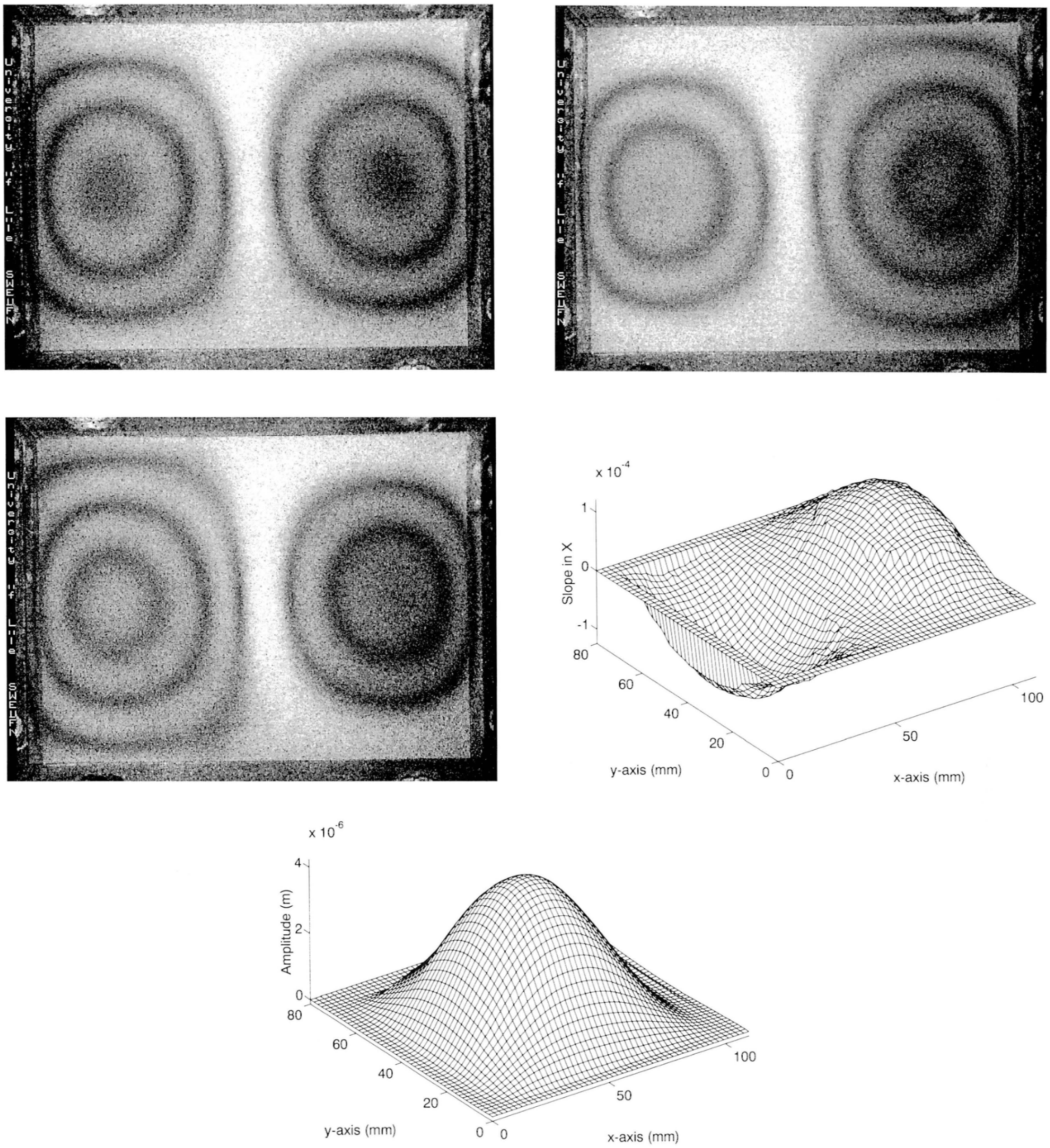

FIGURE 6 Modal analysis of an edge-clamped aluminum plate using electronic shearography (ES). The plate is vibrating at its first eigenfrequency at 600 Hz with one antinode at the center of the plate. (a) Fringe pattern produced during the time-average recording of the plate with a horizontally shear. (b) The same as in (a) but with a positive bias modulation and (c) with negative bias modulation. (d) A 3-dimensional plot of the slope change of the vibration amplitude along the x direction, computed from the images shown in Fig. 6(a), (b), and (c). (e) The vibration amplitude field evaluated by numerical integration of Fig. 6(d).

PZM1, and a bias modulation mirror, PZM2, placed in the arms of a Michelson interferometer configuration. A zoom video lens in the front is used along with relay lenses (R) before and after the Michelson interferometer. Initially both mirrors are adjusted so that one overlapped image is formed. Shear in any desired direction can be introduced in the image by tilting the PZM2. For vibration studies, the PZM2 can then be driven to provide bias vibration. The two laterally sheared wave fronts interfere with each other on the target of the CCD camera. The electrical parts of the system are the same as in EH [Fig. 2(b)].

The shearography optical arrangement is less sensitive to environmental disturbances than ordinary EH. The reason for that is the quasiequal pathway for the two interfering images. The use of ES in modal analysis also extends the measuring range of the amplitude of vibration because the sensitivity depends on the shear distance between the interfering images that can be set, respectively. Figure 6(a)–(c) shows the three interferograms used to produce a numerical evaluation of the measured slope change. A small bias modulation introduces a phase shift of $\pm\pi/3$ in Fig. 6(b) and (c) via the PZM2. By postprocessing, the measured slope change is quantified [Fig. 6(d)]. If the amplitude of the vibration is searched, simple and stable numerical integration gives the out-of-plane deformation field [see Fig. 6(e)]. The calibrated exciter is needed to compare the result with other experiments or calculations.

CONCLUSION

Reciprocity was used to calibrate the force of noncontacting exciters. Two different types of exciters were investigated experimentally. Both types work as point exciters and will not drive vibration modes with nodal lines close to the position of the exciter. The present exciters were not compared with other types. The first type uses a small permanent magnet fastened onto the object surface and a fixed coil that, via an air gap, gives the excitation force. For a small gap between the coil and the permanent magnet, the force from the exciter becomes quite nonlinear. The smallest working distance for one coil/permanent magnet combination was determined to be about 1.5 mm. These type of exciters can be used for nonconducting materials like wood and polymer composites. The amplitude of the force was calibrated and a typical value was 1/100 N.

The second type of exciter uses the eddy-current effect and can be used for objects made of a conducting material. A coil introduces eddy currents into the object by inductance. The interaction between these eddy currents in the object and the stationary electromagnetic field from a permanent magnet give rise to the force in the object. These type of exciters are true noncontact ones, have no mass loading of the object, and are recommended for objects made of a conducting material. The force depends on the material, the thickness of the object, and the distance d between the object and the exciter. The amplitude of the force was calibrated and determined to about 2/100 N for 0.7-mm aluminum. For a thickness of 2.0 mm, the force gets 2.2 times stronger.

The author wishes to thank Dr. Bo Kjellmert for helpful discussions about the electrodynamics of the exciters, and my supervisor Professor Nils-Erik Molin for his support. This work was supported by the Swedish Research Council for Engineering Sciences (TFR).

REFERENCES

Ewins, D. J., 1984, *Modal Testing: Theory and Practice*, Research Studies Press, Letchworth, UK.

Fung, Y. C., 1965, *Foundations of Solid Mechanics*, Prentice–Hall Inc., Englewood Cliffs, NJ, p. 5.

Hung, Y. Y., 1974, "A Speckle-Shearing Interferometer: A Tool for Measuring Derivatives of Surface Displacement," *Optics Communications*, Vol. 11, pp. 132–135.

Jackson, J. D., 1975, *Classical Electrodynamics*, Wiley, New York, p. 298.

Jansson, E. V., Molin, N.-E., and Saldner, H. O., 1994, "On Eigenmodes of the Violin—Electronic Holography and Admittance Measurements," *Journal of the Acoustics Society of America*, Vol. 95, pp. 1100–1105.

Løkberg, O. J., "Recent Development in Video Speckle Interferometry," in R. S. Sirohi, *Speckle Metrology*, 1993, Marcel Dekker, New York, pp. 157–194.

Mohan, N. K., Saldner, H., and Molin, N.-E., 1994, "Electronic Shearography Applied to Static and Vibrating Objects," *Optics Communications*, Vol. 108, pp. 197–202.

Stetson, K. A., 1990, "Theory and Applications of Electronic Holography," *Proceedings of the SEM*, Baltimore, MD, pp. 294–300.

Stetson, K. A., and Brohinsky, W. R., 1988, "Fringe-Shifting Technique for Numerical Analysis of Time-Average Holograms of Vibration Objects," *Journal of the Optical Society of American A*, Vol. 5, pp. 1472–1476.

Stetson, K. A., Brohinsky, W. R., Wahid, J., and Bushman, T., 1989, "An Electro-Optic Holography System with Real-Time Arithmetic Processing," *Journal of Non-Destructive Evaluations,* Vol. 8, pp. 69–76.

Thomson, W. T., 1988, *Theory of Vibration with Applications,* 3rd ed., Unwin Hyman Ltd., London, Chap. 3.10.

Wolde, T. T., 1973, "On the Validity and Application of Reciprocity in Acoustical, Mechano-Acoustical and Other Systems," *Acustica,* Vol. 28, pp. 23–32.